

Article

Surface Modification on Cellulose Nanofibers by TiO₂ Coating for Achieving High Capture Efficiency of Nanoparticles

Chenning Zhang, Tetsuo Uchikoshi * , Izumi Ichinose and Lihong Liu

Research Center for Functional Materials, National Institute for Materials Science, Tsukuba 3050047, Japan; ZHANG.Chenning@nims.go.jp (C.Z.); ICHINOSE.Izumi@nims.go.jp (I.I.); LIU.Lihong@nims.go.jp (L.L.)

* Correspondence: UCHIKOSHI.Tetsuo@nims.go.jp; Tel.: +81-29-859-2460

Received: 4 January 2019; Accepted: 18 February 2019; Published: 20 February 2019



Abstract: Cellulose nanofibers were modified by TiO₂ gel layer (~25 nm in thickness) via hydrolysis reaction on the surface of the cellulose nanofibers. After the TiO₂ coating, the surface charge of the nanofiber dramatically changed from negative to positive. A high efficiency (~100%) of capturing negatively charged Au nanoparticles (5 nm) was successfully obtained by effectively utilizing the electrostatic interaction of surface charge between the TiO₂-coated cellulose nanofibers and Au nanoparticles. Therefore, this technique of surface modification will be potentially used in improving filtration efficiency for membrane applications.

Keywords: cellulose nanofibers; TiO₂ coating; electrostatic interaction; filtration

1. Introduction

The membrane filtration technique has attracted much attention in broad application regions involving food technology, biotechnology, the pharmaceutical industry, and wastewater treatment, and has been known to be superior to conventional thermal separation techniques [1,2]. A synthetic membrane can be prepared from a large number of different inorganic and organic materials, generally including metal, ceramic, and polymer [3]. Cellulose, which is most naturally abundant on earth and found in green plants, wood, cotton, and other planted materials, is light (1.5 g/cm³), tough, and soft. It is one of the commonly known polymers and organized as a network of microfibers used for fabricating membrane as a primitive and traditional raw material [4].

To improve the performance of cellulose or make it applicable to some specific uses, the surface modification of cellulose is generally employed and has been reported in literature, e.g., cellulose nanopapers after being modified by adsorption of polymer, such as moisture buffers [5], microfibrillated cellulose after the surface modification of aminosilane to obtain better mechanical properties [6], cellulose nanocrystals grafted with polystyrene chains to improve capacity of pollutant absorption [7]. Interestingly, except polymer modifications mentioned above, coating cellulose uniformly with ultrathin metal oxide gel layer has been successfully achieved by using a surface sol-gel process via a layer-by-layer deposition technique. Typically, Huang et al. [8–10] reported a surface sol-gel process to prepare metal oxides of ZrO, SnO₂, and TiO₂ with nano-precision replication of natural cellulosic substance. Later, based on this strategy, they coated hierarchical cellulose nanofibers with titania-gel layers in nanometer thickness as biomolecular modification and effectively achieved abundant immobilization of protein molecules [11].

Recently, effective separation of nanoscaled substances, like viruses, proteins, microbes, and organics, has been highly demanded in biomedicine [12], pure water treatment [13], and the pharmaceutical industry [14]. For the cellulose nanofiber as a promising component material of

filtration membrane, the improvement of capture efficiency of a nanofiber surface has been known as one of the dominant factors that prevail over the whole separation performance for filtration membrane.

Therefore, based on the strategy of preparing ultrathin gel layer of metal oxide by utilizing adsorption of metal alkoxides from a solution and the subsequent hydrolysis of the chemisorbed alkoxides [15,16], in this work, a continuous ultrathin layer of TiO₂ gel was successfully coated around cellulose nanofibers. After the TiO₂ layer coating, nanoparticles of 5 nm, which almost equals to the size of a virus, were found to be proficiently captured by the TiO₂-coated cellulose nanofibers that acted as adsorbents; and the mechanism of the significantly improved capture efficiency was systematically investigated.

2. Materials and Methods

2.1. Preparation of TiO₂-Coated Cellulose Nanofibers

Two grams of the as-received cellulose nanofibers (BiNFi-s cellulose nanofibers, 2 wt.% concentration stocked in aqueous media, WMa-10002, Sugino Machine Ltd., Toyama, Japan) were dispersed into a TiO₂ precursor under stirring for 24 h. The TiO₂ precursor was prepared by mixing 40 mL of ethanol (C₂H₅OH) (99.5% purity, Nacalai Tesque Inc., Kyoto, Japan) as a solvent, 2 mL of titanium (IV) tetrabutoxide (Ti(OC₄H₉)₄, TTBO) (Wake Pure Chemical Industries, Ltd., Osaka, Japan) as a titanium source, and 1.85 mL of diethanolamine (HN(OC₂H₅)₂, DEA) (Wake Pure Chemical Industries, Ltd., Osaka, Japan) at a molar ratio of TTBO:DEA = 1:3. Herein, DEA was used as a reagent to suppress serious hydrolysis of TTBO reacting with H₂O that was from an aqueous solvent of the cellulose nanofibers. However, in order to allow slight hydrolysis of the chemisorbed TTBO we proceeded to form a continuous gel layer of TiO₂ coating around the cellulose nanofibers. After the coating, the TiO₂-coated cellulose nanofibers were collected by centrifugation separation, washed with ethanol three times and then reserved in aqueous media.

2.2. Evaluation of Capture Efficiency for Au Nanoparticles

Six milliliters of commercial Au colloidal aqueous suspension (BBIInternational, gold colloid: 5 nm, concentration: 5.81×10^{-9} mol/L, and solvent: water, BBI Solutions OEM Ltd., Crumlin, UK) was added into the prepared TiO₂-coated cellulose nanofibers that were contained in aqueous media under continuous stirring for 1 h. The Au colloids with a particle size of 5 nm and zeta potential of approximately -27 mV, were used to simulate a nanosized virus with a negative charge in water [17,18]. In order to capture the Au nanoparticles, the mixed suspension of Au nanoparticles and TiO₂-coated cellulose nanofibers was filtrated by employing the suction filtration method, as exhibited in Figure S1.

The filtrated suspension was collected and then measured by UV-Vis spectroscopy. The intensity of absorption peak at ~ 520 nm from the Au nanoparticles that remained in the filtrated suspension was used to evaluate the capture efficiency of the Au nanoparticles by the TiO₂-coated cellulose nanofibers. Comparatively, the as-received cellulose nanofibers were also used to capture Au nanoparticles by using suction filtration under the same conditions mentioned above.

2.3. Characterizations

Phase identification was performed by X-ray diffraction (XRD) on an X-ray diffractometer (model RINT 2200, Rigaku Corp., Tokyo, Japan) with nickel-filtered Cu K α radiation at 40 kV and 40 mA operation and a scanning speed of $2\theta = 4^\circ/\text{min}$. Fourier transform infrared (FT-IR) spectra were recorded by FT-IR spectroscopy (model 4200, JASCO, Tokyo, Japan), using the standard KBr method. Morphology and cross-section were observed by a field-emission scanning electron microscopy (FE-SEM) (model S-4800, Hitachi, Ltd., Tokyo, Japan). Element mapping was detected by an energy dispersive X-ray (EDX) spectrometer (model EDAX Apollo XL, EDAX Inc., Mahwah, NJ, USA). Zeta potential and pH were measured by a zeta potential analyzer (model Zetasizer Nano Z, Malvern Instrument Ltd., Malvern, Worcestershire, UK) and a pH meter (model ss973, Horiba, Ltd., Kyoto,

Japan) with a pH electrode (model 6261, Horiba, Ltd., Kyoto, Japan), respectively. Absorption spectra of the filtrated suspension were measured by ultraviolet-visible light (UV-Vis) spectroscopy on a spectrophotometer (Jasco V-570, Jasco Corp., Hachioji, Tokyo, Japan).

3. Results

Figure 1 exhibits (a) XRD patterns and (b) FT-IR spectra of the cellulose nanofibers without and with the TiO₂ coating. As demonstrated in the XRD patterns (Figure 1a), some unresolved XRD peaks were observed for the cellulose nanofibers owing to their low crystallinity but are still identified by referring JCPDS-ICDD:50-2241. Comparatively, after the TiO₂ coating, these XRD peaks became more unresolved, due to the surface of cellulose nanofibers covered by amorphous TiO₂ gel. In the FT-IR spectra (Figure 1b), for the cellulose nanofiber, a wide band in the region between 3575 and 3210 cm⁻¹ was specified as a free O–H stretching vibration of OH groups in the cellulose molecules [19], a characteristic C–H stretching vibration appeared at around 2899 cm⁻¹ [20]. The vibration peak detected at 1637 cm⁻¹ was related to the O–H bending vibration of adsorbed water [21]. The peaks between 1160 and 1015 cm⁻¹ were assigned to a C–O–C asymmetric stretching vibration at the β–glucosidic linkage in a cellulose chain [22], and the peak at 897 cm⁻¹ was associated with the glycosidic linkage between glucose units in cellulose [23]. Regarding the TiO₂-coated cellulose, the features of functional group of hydroxyl (OH) and carbonaceous presented at a wavenumber ranging from 3500 to 2800 cm⁻¹ and 1700 to 1300 cm⁻¹ [24,25], and the fingerprint of Ti–O bond was corresponding to the peaks located between 800 to 400 cm⁻¹ [26].

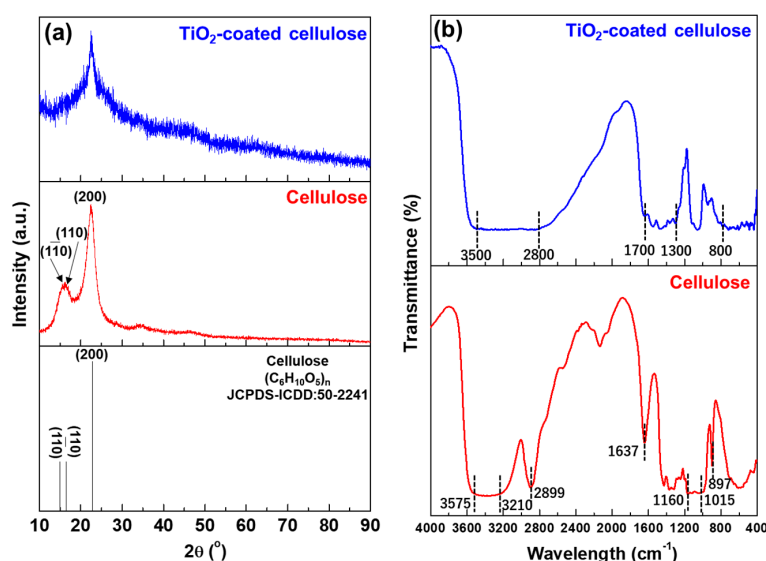


Figure 1. (a) XRD patterns and (b) FT-IR spectra of the cellulose nanofibers before and after the TiO₂ coating.

Figure 2 demonstrates the FE-SEM micrographs of (a) the morphology of a single TiO₂-coated cellulose nanofiber with a locally enlarged image and its EDX element mapping, and (b) the layer thickness of the TiO₂ coating estimated from a cross-section image of the TiO₂-coated cellulose nanofiber. As seen from Figure 2a, the single cellulose nanofiber has ~10 μm in width and ~500 μm in length. Moreover, from the locally enlarged image in Figure 2a, it was observed that the surface of the cellulose nanofiber became rough after the TiO₂ coating, unlike the case of the smooth surface in the uncoated cellulose nanofiber (Figure S2), and the surface element composition of the TiO₂-coated cellulose nanofiber was detected as C, O, and Ti by the EDX element mapping. In addition, the thickness of the TiO₂ coating layer was estimated from the cross-section observation of the TiO₂-coated cellulose nanofiber (Figure 2b) as ~25 nm.

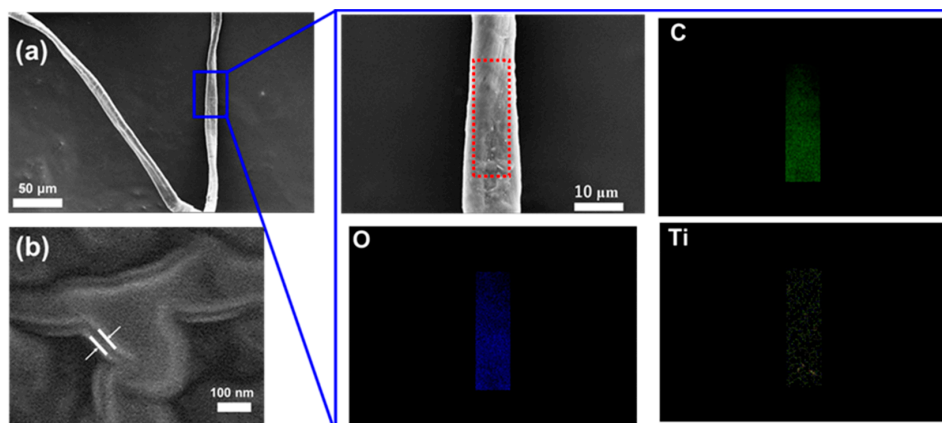


Figure 2. FE-SEM micrographs of (a) morphology of a single TiO₂-coated cellulose nanofiber with a locally enlarged image and EDX element mapping and (b) a cross-section observation of the TiO₂-coated cellulose nanofiber.

The UV-vis spectra of the suspensions before and after filtration using cellulose nanofibers and TiO₂-coated cellulose nanofibers are shown in Figure 3 including (a) UV-Vis spectra of the Au colloidal suspensions before and after the filtration using uncoated and TiO₂-coated cellulose nanofibers, (b) the photographs of color appearances in the Au colloidal suspension, and (c) filtrated uncoated and TiO₂-coated cellulose nanofibers. Based on the intensities of absorption peaks at ~520 nm before and after the filtration (Figure 3a), the capture efficiency of the Au nanoparticles of the cellulose nanofiber is ~47%. In contrast, the capture efficiency was significantly improved up to nearly 100% after the TiO₂ coating. Such significant improvement in the capture efficiency of the Au nanoparticles was also observed in quite different color appearances of the Au colloidal suspensions before and after the filtration (Figure 3b). After the filtration, the wine-like color of the Au colloidal suspension became pale when using the cellulose nanofiber, but appreciably, turned to almost colorless, water-like when employing TiO₂-coated cellulose nanofiber. Furthermore, high capture efficiency of the Au nanoparticles was also conceived from the images of filtrated cellulose nanofibers with and without the TiO₂ coating (Figure 3c). Dark purple in the TiO₂-coated cellulose nanofibers indicates that more Au nanoparticles were effectively captured onto the surface of the nanofibers as a contribution from the TiO₂ gel layer, compared with light-purple color of the uncoated cellulose nanofibers.

Figure 4 demonstrates (a) FE-SEM micrograph of a single TiO₂-coated cellulose nanofiber after filtrating Au colloidal suspension, with (b) EDX element mapping upon its surface, and (c) a schematic illustration showing the mechanism of high capture efficiency of the Au nanoparticles after the TiO₂ coating. After the filtration, it is quite difficult to distinguish the existence of the filtrated Au nanoparticles on the surface of the TiO₂-coated cellulose nanofiber from Figure 4a, due to the nanosize (5 nm) of Au particles. For this reason, element mapping was employed upon a local surface area of the coated nanofiber after the filtration by EDX element mapping. The EDX mapping not only detected the component elements of C and O from the cellulose and coating elements of Ti from the TiO₂ coating layer, but also distinguishably evidenced the existence of Au elements at the nanofiber surface. This indicates that the Au nanoparticles were efficiently captured at the surface of the TiO₂-coated cellulose nanofibers. To understand the highly effective capture of the Au nanoparticles achieved after the TiO₂ coating, a schematic illustration was used to explain the capture mechanism of the Au nanoparticles during the filtration in Figure 4b,c. Based on the theory of electrostatic interactions from surface charges [27], for the cellulose nanofibers, their negative surface charge (zeta potential = −12 mV measured at pH = 8.49) made them strongly repulse the Au nanoparticles (zeta potential = −27 mV measured at pH = 8.45) and, therefore, lowered the filtration efficiency. After the TiO₂ coating, the zeta potential of the cellulose nanofibers turned to +32 mV measured at pH = 8.47, resulting in effective adsorption of the negatively charged Au nanoparticles onto the positive-charged surface of the

TiO₂-coated cellulose nanofiber, and hence enhanced the capture efficiency. Similar research concerning the electrostatic interactions utilized in the membranes, that has also been found elsewhere, reveals that the influence of positively or negatively charged filtration substance and membrane on filtration performance [28–32]. In particular, Breite et al. [33] reported that electrostatic attractive/repulsive interactions play a role in the oppositely/evenly charged membrane surface and fouling reagent as a dominant driving force by tailoring membrane surface charge.

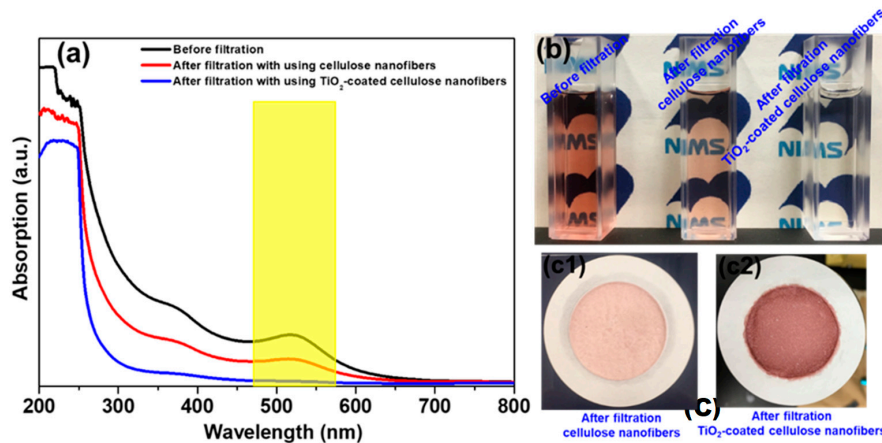


Figure 3. (a) UV-vis spectra of the Au colloidal suspensions before and after filtration using uncoated and TiO₂-coated cellulose nanofibers, and (b) their photographs of color appearances in the Au colloidal suspensions and (c) filtrated cellulose nanofibers without and with TiO₂ coating.

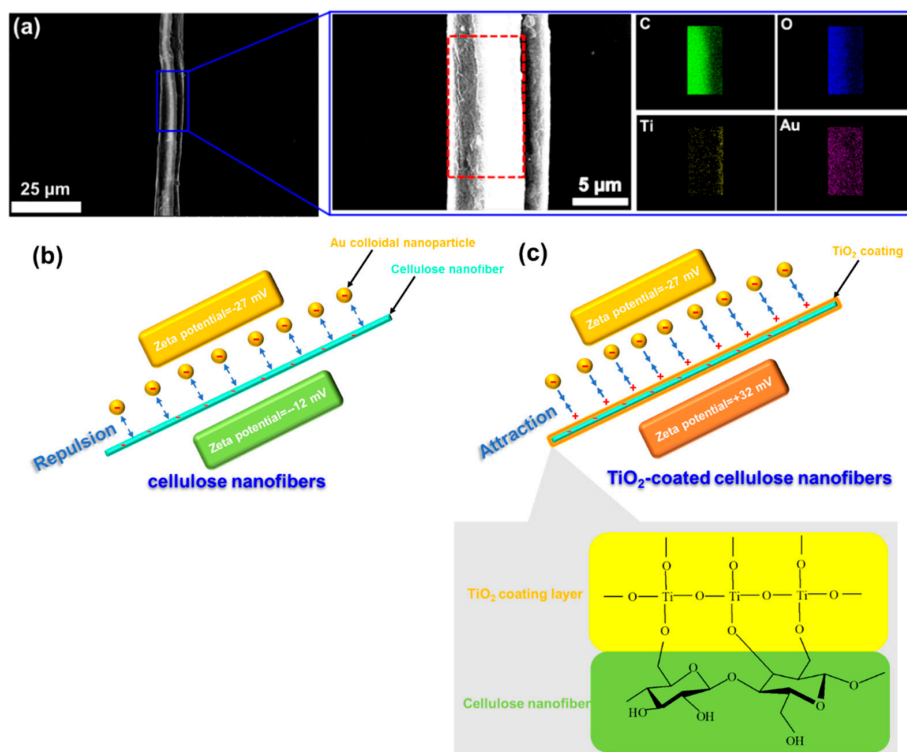


Figure 4. (a) FE-SEM micrograph of a single TiO₂-coated cellulose nanofiber after filtrating Au colloidal suspension, with a locally enlarged FE-SEM image and EDX element mapping, (b) and (c) a schematic illustration explaining the mechanism of electrostatic interaction to achieve a high capture efficiency for the Au nanoparticles after the TiO₂ surface coating.

4. Conclusions

A coating layer of amorphous TiO₂ (~25 nm in thickness) was prepared around cellulose nanofibers by hydrolyzing TiO₂ precursor chemisorbed on the surface of cellulose. The surface of the cellulose nanofiber changed from smooth to rough after the TiO₂ modification, and interestingly, the surface charge was changed from negative to positive. The TiO₂-coated cellulose nanofibers as adsorbent gave a significantly high capture efficiency (~100%) for the Au nanoparticles (5 nm), much higher than that (~47%) by using the uncoated cellulose nanofibers, by effectively utilizing the electrostatic interaction between the negatively charged Au nanoparticles and positively charged cellulose nanofibers after the TiO₂ surface modification.

Supplementary Materials: The following are available online at <http://www.mdpi.com/2079-6412/9/2/139/s1>, Figure S1: Photographs of (a) TiO₂-coated cellulose nanofibers stocked in aqueous media, (b) after adding Au nanoparticles, (c) on-going filtration to capture Au nanoparticles, and (d) Au nanoparticles captured by the TiO₂-coated cellulose nanofibers after the filtration; Figure S2: FE-SEM micrograph showing morphology of the cellulose nanofibers without the TiO₂ coating.

Author Contributions: Writing—Original Draft Preparation, C.Z.; Writing—Review and Editing, T.U.; Supervision, T.U.; Project Administration, I.I.; Formal Analysis, L.L.

Funding: This research received no external funding.

Conflicts of Interest: The authors declare no conflict of interest.

References

1. Osada, Y.; Nakagawa, T. *Membrane Science and Technology*; Marcel Dekker: New York, NY, USA, 1992.
2. Baker, R.W. *Membrane Technology and Applications*, 2nd ed.; Wiley: West Sussex, UK, 2004.
3. Perry, R.H.; Green, D.W.; Maloney, J.O. *Perry's Chemical Engineers' Handbook*; McGraw-Hill: New York, NY, USA, 1997.
4. Hilal, N.; Ismail, A.F.; Wright, C. *Membrane Fabrication*, 1st ed.; CRC Press: Boca Raton, FL, USA, 2015.
5. Kontturi, K.S.; Biegaj, K.; Mautner, A.; Woodward, R.T.; Wilson, B.P.; Johansson, L.S.; Lee, K.Y.; Heng, J.Y.Y.; Bismarck, A.; Kontturi, E. Noncovalent surface modification of cellulose nanopapers by adsorption of polymers from aprotic solvents. *Langmuir* **2017**, *33*, 5707–5712. [[CrossRef](#)] [[PubMed](#)]
6. Lu, J.; Askeland, P.; Drzal, L.T. Surface modification of microfibrillated cellulose for epoxy composite applications. *Polymer* **2008**, *49*, 1285–1296. [[CrossRef](#)]
7. Morandi, G.; Heath, L.; Thielemans, W. Cellulose nanocrystals grafted with polystyrene chains through surface-initiated atom transfer radical polymerization (SI-ATRP). *Langmuir* **2009**, *25*, 8280–8286. [[CrossRef](#)]
8. Huang, J.; Kunitake, T. Nano-precision replication of natural cellulosic substances by metal oxides. *J. Am. Chem. Soc.* **2003**, *125*, 11834–11835. [[CrossRef](#)]
9. Huang, J.; Matsunaga, N.; Shimano, K.; Yamazoe, N.; Kunitake, T. Nanotubular SnO₂ templated by cellulose fibers: Synthesis and gas sensing. *Chem. Mater.* **2005**, *17*, 3513–3518. [[CrossRef](#)]
10. Huang, J.; Kunitake, T.; Onoue, S.Y. A facile route to a highly stabilized hierarchical hybrid of titania nanotube and gold nanoparticle. *Chem. Commun.* **2004**, 1008–1009. [[CrossRef](#)]
11. Huang, J.; Ichinose, I.; Kunitake, T. Biomolecular modification of hierarchical cellulose fibers through titania nanocoating. *Angew. Chem.* **2006**, *118*, 2949–2952. [[CrossRef](#)]
12. Li, N.N.; Fane, A.G.; Ho, W.S.W.; Matsuura, T. *Advanced Membrane Technology and Applications*; John Wiley & Sons: New York, NY, USA, 2011.
13. Figoli, A.; Hoinkis, J.; Altinkaya, S.A.; Bundschuh, J. *Application of Nanotechnology in Membranes for Water Treatment*; CRC Press: London, UK, 2017.
14. Thakur, V.K.; Thakur, M.K. *Handbook of Polymers for Pharmaceutical Technologies, Processing and Applications*; John Wiley & Sons: New York, NY, USA, 2015.
15. Ichinose, I.; Senzu, H.; Kunitake, T. A surface sol–gel process of TiO₂ and other metal oxide films with molecular precision. *Chem. Mater.* **1997**, *9*, 1296–1298. [[CrossRef](#)]
16. Huang, J.; Ichinose, I.; Kunitake, T. Replication of dendrimer monolayer as nanopores in titania ultrathin film. *Chem. Commun.* **2002**, *18*, 2070–2071. [[CrossRef](#)]

17. Sobsey, M.D.; Jones, B.L. Concentration of poliovirus from tap water using positively charged microporous filters. *Appl. Environ. Microbiol.* **1979**, *37*, 588–595.
18. Michen, B.; Graule, T. Isoelectric points of viruses. *J. Appl. Microbiol.* **2010**, *109*, 388–397. [[CrossRef](#)] [[PubMed](#)]
19. Li, J.; Wang, Y.; Wei, X.; Wang, F.; Han, D.; Wang, Q.; Kong, L. Homogeneous isolation of nanocelluloses by controlling the shearing force and pressure in microenvironment. *Carbohydr. Polym.* **2014**, *113*, 388–393. [[CrossRef](#)] [[PubMed](#)]
20. Khalil, H.A.; Ismail, H.; Rozman, H.D.; Ahmad, M.N. The effect of acetylation on interfacial shear strength between plant fibres and various matrices. *Eur. Polym. J.* **2001**, *37*, 1037–1045. [[CrossRef](#)]
21. Wandlowski, T.; Ataka, K.; Pronkin, S.; Diesing, D. Surface enhanced infrared spectroscopy—Au(111-20 nm)/sulphuric acid—New aspects and challenges. *Electrochim. Acta* **2004**, *49*, 1233–1247. [[CrossRef](#)]
22. Åkerholm, M.; Salmén, L. Interactions between wood polymers studied by dynamic FT-IR spectroscopy. *Polymer* **2001**, *42*, 963–969. [[CrossRef](#)]
23. Liu, Y. Recent progress in fourier transform infrared (FTIR) spectroscopy study of compositional, structural and physical attributes of developmental cotton fibers. *Materials* **2013**, *6*, 299–313. [[CrossRef](#)] [[PubMed](#)]
24. Wu, C.Y.; Chiang, B.S.; Chang, S.; Liu, D.S. Determination of photocatalytic activity in amorphous and crystalline titanium oxide films prepared using plasma-enhanced chemical vapor deposition. *Appl. Surf. Sci.* **2011**, *257*, 1893–1897. [[CrossRef](#)]
25. Lee, W.G.; Won, S.I.; Kim, J.C.; Choi, S.H.; Oh, K.H. Preparation and properties of amorphous TiO₂ thin films by plasma enhanced chemical vapor deposition. *Thin Solid Films* **1994**, *237*, 105–111. [[CrossRef](#)]
26. Tao, P.; Li, Y.; Rungta, A.; Viswanath, A.; Gao, J.; Benicewicz, B.C.; Siegel, R.W.; Schadler, L.S. TiO₂ nanocomposites with high refractive index and transparency. *J. Mater. Chem.* **2011**, *21*, 18623–18629. [[CrossRef](#)]
27. Butt, H.J.; Graf, K.; Kappl, M. *Physics and Chemistry of Interfaces*; Wiley-VCH: Weinheim, Germany, 2006.
28. Pujar, N.S.; Zydney, A.L. Electrostatic and electrokinetic interactions during protein transport through narrow pore membranes. *Ind. Eng. Chem. Res.* **1994**, *33*, 2473–2482. [[CrossRef](#)]
29. Van Eijndhoven, R.H.; Saksena, S.; Zydney, A.L. Protein fractionation using electrostatic interactions in membranel filtration. *Biotechnol. Bioeng.* **1995**, *48*, 406–414. [[CrossRef](#)] [[PubMed](#)]
30. Van Reis, R.; Gadam, S.; Frautschy, L.N.; Orlando, S.; Goodrich, E.M.; Saksena, S.; Kuriyel, R.; Simpson, C.M.; Pearl, S.; Zydney, A.L. High performance tangential flow filtration. *Biotechnol. Bioeng.* **1997**, *56*, 71–82. [[CrossRef](#)]
31. Nghiem, L.D.; Schäfer, A.I.; Elimelech, M. Role of electrostatic interactions in the retention of pharmaceutically active contaminants by a loose nanofiltration membrane. *J. Membr. Sci.* **2006**, *286*, 52–59. [[CrossRef](#)]
32. Cho, J.; Amy, G.; Pellegrino, J. Membrane filtration of natural organic matter: factors and mechanisms affecting rejection and flux decline with charged ultrafiltration (UF) membrane. *J. Membr. Sci.* **2000**, *164*, 89–110. [[CrossRef](#)]
33. Breite, D.; Went, M.; Prager, A.; Schulze, A. Tailoring membrane surface charges: A novel study on electrostatic interactions during membrane fouling. *Polymers* **2015**, *7*, 2017–2030. [[CrossRef](#)]

